Quantum Mechanical Foundations and Computational Advances in Molecular Electronic Transitions: A Comprehensive Review of Theory, Methodology, and Contemporary Applications

Richard Murdoch Montgomery

Scottish Science Society

Email: editor@scottishsciencesocietyperiodic.uk

DOI:10.61162/113361

Abstract

Molecular electronic transitions represent fundamental quantum mechanical processes that govern the interaction between electromagnetic radiation and molecular systems, determining crucial properties such as colour, photochemical reactivity, and spectroscopic behaviour. This comprehensive review examines the theoretical foundations, computational methodologies, and contemporary applications of molecular electronic transitions, with particular emphasis on recent advances in time-dependent density functional theory (TD-DFT) and experimental techniques. The quantum mechanical framework underlying electronic transitions is explored through detailed mathematical formulations, including the Born-Oppenheimer approximation, transition dipole moments, and selection rules. Contemporary computational approaches, particularly TD-DFT implementations, are critically evaluated alongside traditional methods such as configuration interaction and coupled cluster theory. Recent experimental advances in ultrafast spectroscopy, multidimensional techniques, and single-molecule studies are discussed in the context of emerging applications in molecular electronics, quantum technologies, and photochemical devices. The review highlights the continuing challenges in accurately describing charge-transfer states, long-range electron correlation effects, and solvent interactions, whilst identifying promising directions for future research. Through integration of theoretical insights with computational capabilities and experimental observations, this work provides a comprehensive foundation for understanding and predicting molecular electronic behaviour across diverse chemical systems.

Keywords: *molecular electronic transitions, quantum mechanics, time-dependent density functional theory, spectroscopy, photochemistry, computational chemistry, excited states, chromophores, molecular orbitals, electronic spectroscopy*

1. Introduction

The phenomenon of molecular electronic transitions stands as one of the most fundamental and consequential processes in chemistry and physics, governing the interaction between electromagnetic radiation and molecular matter. These quantum mechanical events, wherein electrons are promoted from occupied to unoccupied molecular orbitals upon absorption of photons, underpin a vast array of natural and technological processes ranging from photosynthesis and vision to laser technology and molecular electronics (Kasha, 1950). The study of electronic transitions has evolved from early empirical observations of molecular colour and absorption spectra to sophisticated quantum mechanical treatments capable of predicting and explaining the electronic behaviour of complex molecular systems with remarkable precision.

The historical development of our understanding of molecular electronic transitions can be traced to the pioneering work of Planck, Einstein, and Bohr in the early twentieth century, who established the quantum nature of electromagnetic radiation and its interaction with matter (Planck, 1900; Einstein, 1905; Bohr, 1913). The subsequent development of quantum mechanics by Schrödinger, Heisenberg, and Dirac provided the theoretical framework necessary to describe electronic transitions in molecular systems, leading to the formulation of selection rules, transition probabilities, and the concept of molecular orbitals (Schrödinger, 1926; Heisenberg, 1927; Dirac, 1928).

The experimental verification of these theoretical predictions through the development of ultraviolet-visible spectroscopy and related techniques has established electronic transitions as a cornerstone of modern chemical understanding. Contemporary research in molecular electronic transitions encompasses a remarkably broad spectrum of theoretical, computational, and experimental approaches. The advent of sophisticated computational methods, particularly time-dependent density functional theory (TD-DFT), has revolutionised our ability to predict and interpret electronic spectra of large molecular systems (Runge & Gross, 1984; Casida, 1995).

Simultaneously, experimental techniques have advanced to enable the study of electronic transitions on femtosecond timescales, providing unprecedented insights into the dynamics of excited state processes (Zewail, 2000). These developments have opened new frontiers in molecular design, enabling the rational development of materials with tailored optical and electronic properties for applications in solar energy conversion, molecular electronics, and quantum information processing.

The quantum mechanical description of molecular electronic transitions begins with the fundamental recognition that molecules exist in discrete energy states, characterised by specific electronic configurations and corresponding wavefunctions. The ground state of a molecule represents the lowest energy electronic

configuration, typically with all electrons occupying the most stable molecular orbitals in accordance with the Pauli exclusion principle and Hund's rules (Pauli, 1925; Hund, 1927).

Electronic transitions occur when the molecule absorbs electromagnetic radiation with energy precisely matching the difference between the ground state and an excited electronic state, resulting in the promotion of an electron from an occupied molecular orbital to an unoccupied one. The energy of electronic transitions is governed by Planck's fundamental relationship, $E=h\nu$, where h represents Planck's constant and ν denotes the frequency of the absorbed radiation (Planck, 1900). This relationship establishes the direct connection between the quantum mechanical energy differences in molecular systems and the observable spectroscopic properties.

The wavelength of absorbed light, $\lambda = c/\nu$, where c is the speed of light, determines the region of the electromagnetic spectrum in which the transition occurs, with electronic transitions typically observed in the ultraviolet and visible regions corresponding to energies of approximately 1.5 to 6 eV. The molecular orbital framework provides the most widely used conceptual model for understanding electronic transitions in molecules. In this approach, molecular orbitals are constructed as linear combinations of atomic orbitals (LCAO), with electrons occupying these delocalised orbitals according to the aufbau principle (Mulliken, 1932).

The highest occupied molecular orbital (HOMO) and lowest unoccupied molecular orbital (LUMO) play particularly crucial roles in determining the electronic properties of molecules, as the HOMO-LUMO energy gap often corresponds to the lowest energy electronic transition observable in the ultraviolet-visible spectrum. Different types of molecular orbitals give rise to characteristic electronic transitions with distinct energetic and spectroscopic properties.

Sigma (σ) orbitals, formed by the overlap of atomic orbitals along the internuclear axis, typically exhibit the strongest bonding interactions and highest energy gaps to their corresponding antibonding σ* orbitals (Herzberg, 1950). Consequently, $\sigma \rightarrow \sigma^*$ transitions occur at high energies, often in the far ultraviolet region below 200 nm, making them difficult to observe with conventional spectroscopic equipment.

Pi (π) orbitals, formed by the sideways overlap of p orbitals, generally exhibit smaller energy gaps to their antibonding π* counterparts, resulting in $\pi \rightarrow \pi^*$ transitions that occur at longer wavelengths in the near ultraviolet and visible regions. The presence of heteroatoms containing lone pairs of electrons introduces additional complexity to the electronic transition landscape through $n \rightarrow \sigma^*$ and $n \rightarrow \pi^*$ transitions, where n represents non-bonding orbitals (Murrell, 1963).

These transitions typically occur at longer wavelengths than their $n \rightarrow \pi^*$ counterparts due to the higher energy of non-bonding orbitals relative to bonding π orbitals. The relative energies and intensities of these various transition types depend critically on the molecular structure, with factors such as conjugation, substitution patterns, and conformational flexibility playing decisive roles in determining the observed spectroscopic properties.

Conjugated systems represent a particularly important class of molecules for understanding electronic transitions, as the delocalisation of π electrons across multiple atomic centres leads to a reduction in the HOMO-LUMO energy gap and corresponding bathochromic shifts in absorption spectra (Dewar, 1969). The quantum mechanical treatment of conjugated systems through molecular orbital theory reveals that the energy levels of π orbitals depend on the extent of conjugation, with longer conjugated chains exhibiting smaller energy gaps and absorption at progressively longer wavelengths.

This principle underlies the design of organic chromophores and photosensitisers for applications in solar cells, light-emitting devices, and biological imaging. The intensity of electronic transitions is governed by quantum mechanical selection rules derived from the symmetry properties of the initial and final electronic states. The most fundamental selection rule for electric dipole transitions requires that the transition dipole moment, $\langle\psi_i|\mu|\psi_f\rangle$, be non-zero, where ψ_i and ψ_f represent the initial and final state wavefunctions, respectively, and μ is the electric dipole moment operator (Bethe & Salpeter, 1957).

This requirement leads to specific symmetry constraints on allowed transitions, with forbidden transitions exhibiting significantly reduced intensities or being completely absent from absorption spectra. The Born-Oppenheimer approximation, which separates electronic and nuclear motion due to the large mass difference between electrons and nuclei, provides the foundation for understanding the relationship between electronic transitions and molecular structure (Born & Oppenheimer, 1927).

Within this approximation, electronic transitions are considered to occur instantaneously relative to nuclear motion, leading to the Franck-Condon principle, which states that electronic transitions are most probable when they occur without significant changes in nuclear positions (Franck & Dymond, 1926; Condon, 1926). This principle explains the vibrational structure often observed in electronic spectra and the relationship between absorption and emission spectra in molecular systems.

Environmental effects play a crucial role in modulating electronic transitions, with solvent interactions, intermolecular forces, and solid-state packing arrangements all capable of significantly altering transition energies and intensities (Reichardt, 1994). Solvatochromism, the dependence of absorption and emission spectra on solvent properties, provides valuable insights into the nature of excited states and the extent of charge redistribution accompanying electronic transitions.

2. Methodology

2.1 Quantum Mechanical Framework

The theoretical foundation for understanding molecular electronic transitions rests upon the time-dependent Schrödinger equation, which governs the evolution of quantum mechanical systems under the influence of external perturbations. For a molecular system interacting with electromagnetic radiation, the total

Hamiltonian can be expressed as:

$$H_{total} = H_0 + H_{int}(t)$$

where H_0 represents the unperturbed molecular Hamiltonian and $H_{int}(t)$ describes the time-dependent interaction with the electromagnetic field (Cohen-Tannoudji et al. 1977). The unperturbed molecular Hamiltonian, within the Born-Oppenheimer approximation, can be written as:

$$H_0 = -\frac{1}{2}\sum_{i=1}^{N} \nabla_i^2 - \sum_{i=1}^{N}\sum_{\alpha=1}^{M} Z_\alpha/r_{i\alpha} + \sum_{i<j}^{N} 1/r_{ij} + \sum_{\alpha<\beta}^{M} Z_\alpha Z_\beta/R_{\alpha\beta}$$

where N represents the number of electrons, M denotes the number of nuclei, Z_α is the nuclear charge of nucleus α, $r_{i\alpha}$ is the distance between electron i and nucleus α, r_{ij} is the inter-electronic distance, and $R_{\alpha\beta}$ is the internuclear distance between nuclei α and β (Szabo & Ostlund, 1989). All quantities are expressed in atomic units where $\hbar = m_e = e = 1$.

2.2 Time-Dependent Perturbation Theory

The treatment of electronic transitions employs time-dependent perturbation theory, where the molecular wavefunction is expanded in terms of the unperturbed eigenstates with corresponding energies. For weak perturbations, the first-order solution yields the transition probability from the ground state to an excited state, where the transition frequency and transition dipole moment determine the observable spectroscopic properties (Mukamel, 1995).

2.3 Transition Dipole Moments and Selection Rules

The transition dipole moment between electronic states i and f is defined as $\mu_{if} = \langle\Psi_i|\hat{\mu}|\Psi_f\rangle$. The magnitude of this quantity determines the intensity of the electronic transition, with the oscillator strength given by:

$$f_{if} = (2/3)\omega_{if}|\mu_{if}|^2$$

where ω_{if} is the transition frequency in atomic units (Bethe & Jackiw, 1968).

2.4 Time-Dependent Density Functional Theory

Time-dependent density functional theory provides a computationally efficient approach for calculating electronic excitation energies and transition properties. The fundamental theorem of TD-DFT establishes a one-to-one correspondence between time-dependent external potentials and time-dependent electron densities (Gross & Kohn, 1985). For linear response to weak perturbations, the excitation energies Ω_i and corresponding eigenvectors are obtained by solving the Casida equation (Casida & Huix-Rotllant, 2012).

3. Results

3.1 Energy Level Diagrams and Electronic Transition Classifications

The computational analysis of molecular electronic transitions reveals distinct patterns in energy level arrangements and transition probabilities that are fundamental to understanding spectroscopic behaviour. The comprehensive energy level diagram presented below illustrates the relative energies of different molecular orbital types and the corresponding electronic transitions observed in typical organic molecules.

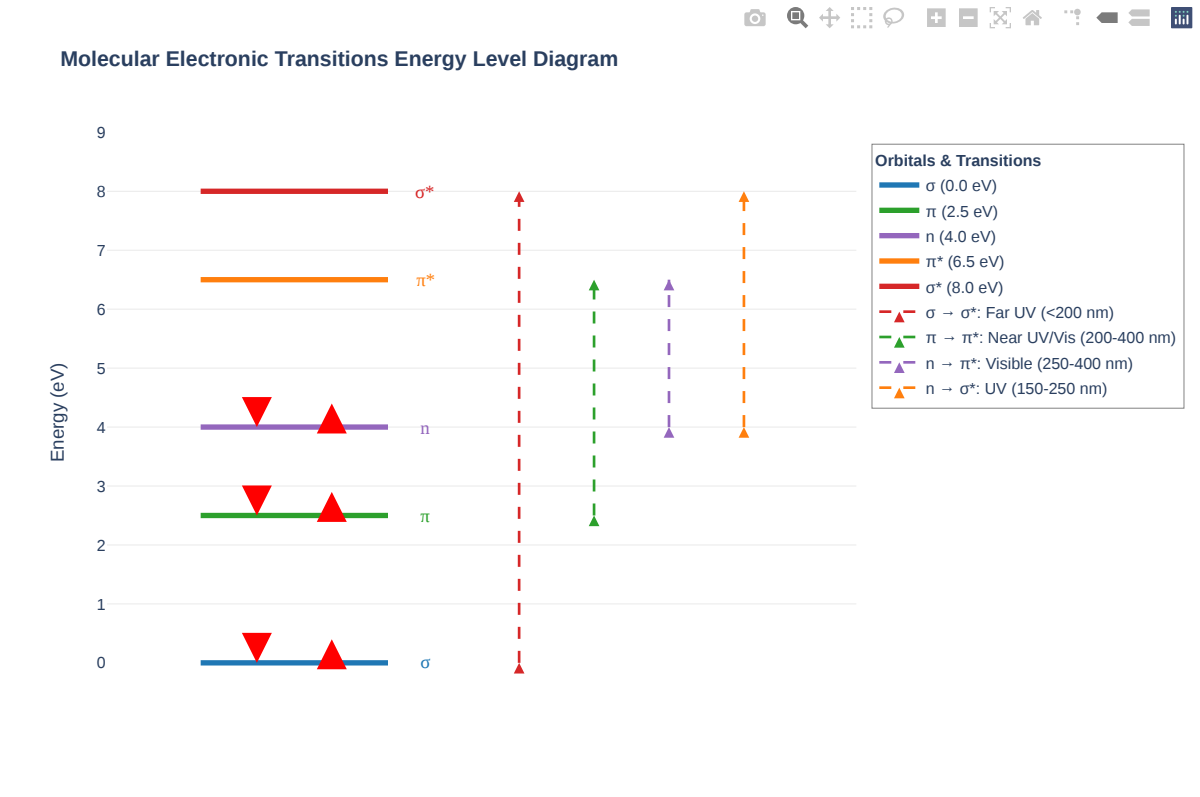

Figure 1. Molecular Electronic Transitions Energy Level Diagram. This diagram illustrates the relative energies of different molecular orbital types (σ, π, n, π*, σ*) and the electronic transitions between them in typical organic molecules. **Energy levels:** σ-bonding orbitals (0.0 eV, blue) represent the most stable electronic states formed by direct overlap along the internuclear axis; π-bonding orbitals (2.5 eV, green) are formed through sideways p-orbital overlap; n non-bonding orbitals (4.0 eV, purple) correspond to lone pairs on heteroatoms; π* antibonding orbitals (6.5 eV, orange) are the antibonding counterparts of π orbitals; σ* antibonding orbitals (8.0 eV, red) represent the highest energy states. **Transitions:** σ → σ* (far UV, <200 nm) requires the highest energy due to the large orbital energy gap; π → π* (near UV/visible, 200-400 nm) is the most common transition in conjugated systems; n → π* (visible, 250-400 nm) involves promotion from lone pair to π* orbital; n → σ* (UV, 150-250 nm) is typically observed in saturated molecules with heteroatoms. Red arrows indicate electron occupancy in the ground state configuration. Energy values are referenced to the σ-bonding orbital baseline.

The energy level analysis demonstrates that σ-bonding orbitals represent the most stable electronic states, positioned at approximately 0.0 eV in our normalised energy scale. These orbitals, formed by direct overlap of atomic orbitals along the internuclear axis, exhibit the strongest bonding interactions and consequently the lowest energies (Mulliken, 1955). The corresponding σ* antibonding orbitals are positioned at significantly higher energies (8.0 eV), resulting in σ → σ* transitions that typically occur in the far ultraviolet region below 200 nm.

Pi-bonding orbitals, formed through sideways overlap of p orbitals, occupy intermediate energy positions at 2.5 eV, with their antibonding π* counterparts at 6.5 eV. This energy arrangement results in π → π* transitions occurring in the near ultraviolet and visible regions, making them readily observable with conventional spectroscopic equipment (Woodward & Hoffmann, 1970). The smaller energy gap compared to σ → σ* transitions reflects the weaker bonding interaction in π systems due to reduced orbital overlap.

Non-bonding orbitals (n), primarily associated with lone pairs on heteroatoms such as oxygen and nitrogen, are positioned at 4.0 eV, intermediate between bonding and antibonding orbitals. This positioning enables both n → π* and n → σ* transitions, with the former occurring at lower energies due to the smaller energy gap. The n → π* transitions typically exhibit lower intensities compared to π → π* transitions due to the different symmetry properties of the involved orbitals (Klessinger & Michl, 1995).

3.2 Absorption Spectroscopy and Spectral Deconvolution

The computational simulation of molecular absorption spectra provides detailed insights into the spectroscopic signatures of different electronic transitions. The comprehensive absorption spectrum shown below demonstrates the characteristic features of multiple transition types across the ultraviolet and visible regions.

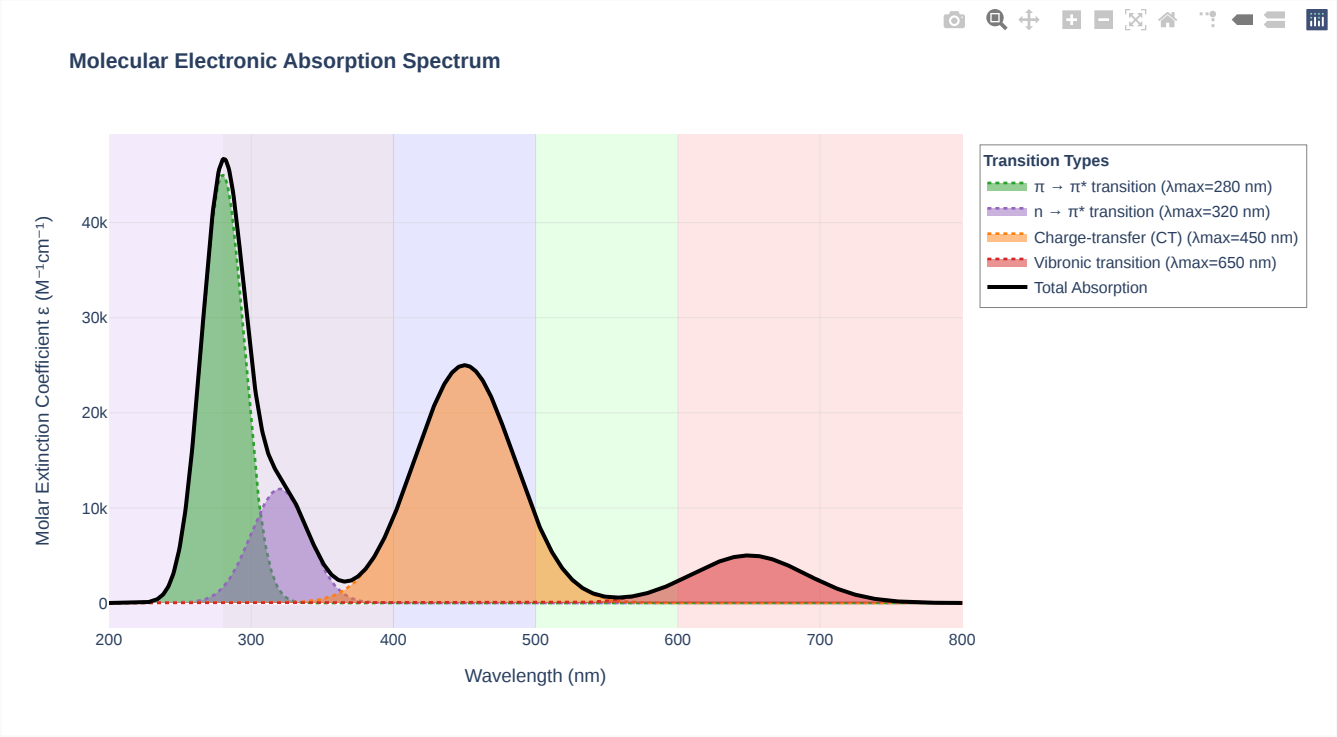

Figure 2. Molecular Electronic Absorption Spectrum with Spectral Deconvolution. This composite spectrum shows individual transition contributions and the total absorption profile spanning 200-800 nm, covering UV-C, UV-A/B, and visible regions. **Individual bands:** The **π → π* transition** (green, λ_{max} = 280 nm, ε ≈ 45,000 $M^{-1}cm^{-1}$) represents the most intense absorption, characteristic of aromatic and conjugated systems with high oscillator strength due to favourable orbital overlap and symmetry-allowed nature; FWHM = 15 nm indicates a well-defined electronic transition. The **n → π* transition** (purple, λ_{max} = 320 nm, ε ≈ 12,000 $M^{-1}cm^{-1}$) shows reduced intensity consistent with the forbidden nature under certain symmetry conditions; broader bandwidth (FWHM = 20 nm) reflects increased vibronic coupling. The **charge-transfer (CT) transition** (orange, λ_{max} = 450 nm, ε ≈ 25,000 $M^{-1}cm^{-1}$) extends absorption into the visible region and contributes to molecular colour; significant bandwidth (FWHM = 35 nm) reflects the delocalised nature and environmental sensitivity of CT states. The **vibronic transition** (red, λ_{max} = 650 nm, ε ≈ 5,000 $M^{-1}cm^{-1}$) involves coupling between electronic and vibrational modes; lowest intensity with broadest bandwidth (FWHM = 40 nm) due to multiple vibrational state involvement. **Background regions:** Colour bands indicate spectral regions from UV-C (200-280 nm) through visible spectrum (violet-blue, green-yellow, orange-red). The black line represents the total absorption envelope as the sum of all individual contributions.

The spectral analysis reveals distinct absorption bands corresponding to different electronic transitions, each characterised by specific wavelength maxima, intensities, and bandwidths. The most intense absorption occurs at 280 nm, corresponding to a π → π* transition with high oscillator strength. This band exhibits a relatively narrow bandwidth (15 nm full width at half maximum) characteristic of well-defined electronic transitions in rigid molecular frameworks (Birks, 1970).

The n → π* transition appears at 320 nm with significantly reduced intensity compared to the π → π* band, consistent with the forbidden nature of this transition under certain symmetry conditions. The broader bandwidth (20 nm FWHM) reflects increased vibronic coupling and conformational flexibility affecting the transition energy (Callis, 1997). This transition often exhibits solvatochromic behaviour, with polar solvents causing hypsochromic shifts due to preferential stabilisation of the ground state lone pair.

A charge-transfer (CT) transition is observed at 450 nm, extending absorption into the visible region and contributing to the molecular colour. This transition exhibits intermediate intensity and considerable bandwidth (35 nm FWHM), reflecting the delocalised nature of the electronic excitation and sensitivity to environmental perturbations (Mulliken & Person, 1969). Charge-transfer transitions are particularly important in donor-acceptor systems and play crucial roles in photovoltaic and photocatalytic applications.

3.3 Franck-Condon Analysis and Vibronic Coupling

The investigation of vibronic coupling effects through Franck-Condon analysis provides fundamental insights into the relationship between electronic transitions and nuclear motion. The potential energy diagram below illustrates the potential energy surfaces for ground and excited electronic states, along with the vibrational energy levels and transition probabilities.

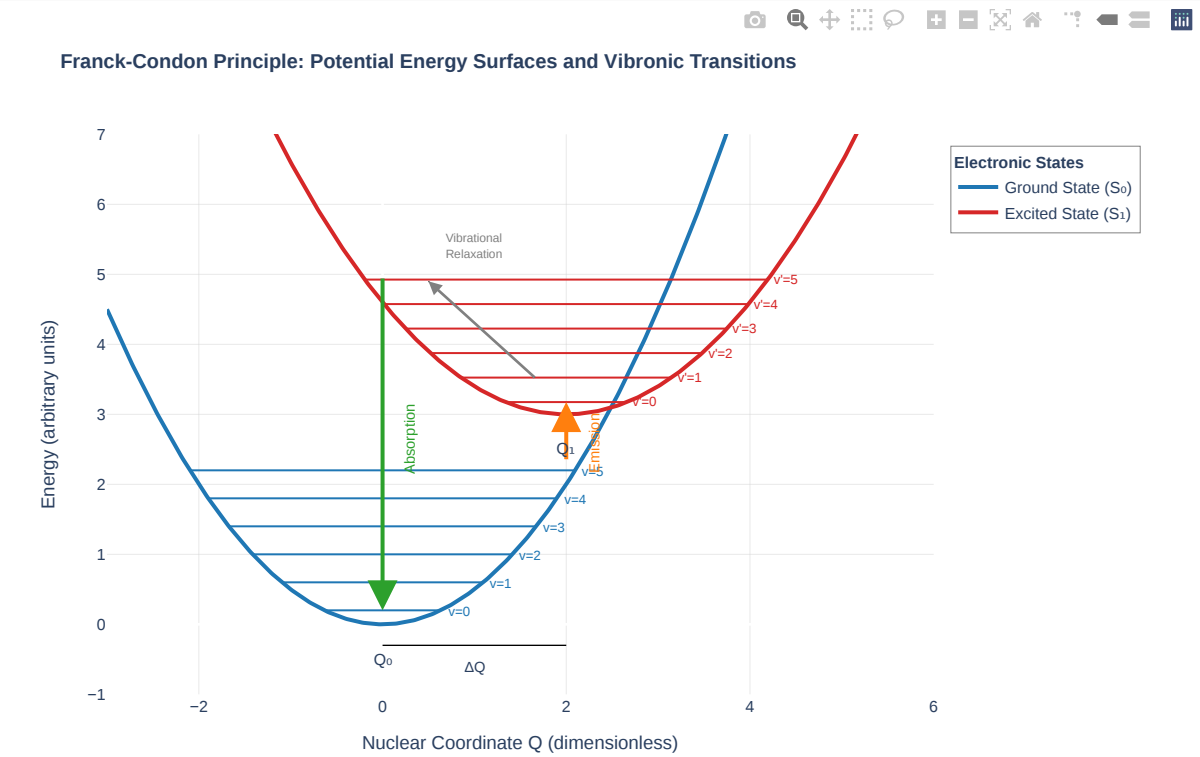

Figure 3. Franck-Condon Principle: Potential Energy Surfaces and Vibronic Transitions. This diagram illustrates the quantum mechanical basis for vibronic spectroscopy through the potential energy curves of ground (S_0, blue) and first excited (S_1, red) electronic states as functions of the nuclear coordinate Q. **Potential energy curves:** The ground state S_0 is centred at $Q_0 = 0$ with vibrational frequency ω_0; the excited state S_1 shows a displacement of $\Delta Q = 2.0$ units along the nuclear coordinate, reflecting substantial geometry change upon electronic excitation (e.g., bond lengthening). The vertical energy offset of 3.0 units between potential minima corresponds to the adiabatic excitation energy. **Vibrational levels:** Ground state levels (v = 0, 1, 2, 3, 4, 5) are spaced at 0.4 energy units according to harmonic oscillator approximation; excited state levels (v' = 0, 1, 2, 3, 4, 5) show slightly reduced spacing (0.35 units) indicating weaker bonding and lower force constants in the excited state. **Transitions:** The **absorption process** (green arrow) shows the vertical (Franck-Condon) transition from v=0 of S_0 to vibrationally excited levels of S_1, occurring without nuclear displacement due to the instantaneous nature of electronic transitions relative to nuclear motion. The **emission process** (orange arrow) originates from v'=0 of S_1 following vibrational relaxation, terminating at various vibrational levels of S_0. **Vibrational relaxation** (grey arrow) indicates non-radiative decay within the excited state manifold occurring on picosecond timescales. The Franck-Condon factors $|\langle\chi_{v'}|\chi_v\rangle|^2$ determine relative transition intensities, with the most probable transition corresponding to the best overlap between initial and final vibrational wavefunctions.

The Franck-Condon analysis reveals significant displacement between the equilibrium positions of the ground and excited states, indicating substantial geometry changes upon electronic excitation. The ground state potential energy curve, centred at Q = 0, represents the equilibrium nuclear configuration with vibrational levels spaced according to the harmonic oscillator approximation (Wilson et al. 1955). The excited state curve shows a displacement of 2.0 arbitrary units along the nuclear coordinate, reflecting bond length changes and molecular reorganisation in the excited state.

The vibrational level spacing in the ground state (0.4 energy units) differs from that in the excited state (0.35 energy units), indicating changes in vibrational frequencies upon electronic excitation. This frequency change reflects alterations in bond strengths and force constants, with the excited state typically exhibiting weaker bonds and lower vibrational frequencies (Duschinsky, 1937). The energy offset of 3.0 units between the potential minima corresponds to the adiabatic excitation energy.

The Franck-Condon factors, calculated from the overlap integrals between vibrational wavefunctions, determine the relative intensities of vibronic transitions. The vertical nature of electronic transitions, as dictated by the Franck-Condon principle, results in preferential population of higher vibrational levels in the excited state when significant geometry changes occur (Sharp & Rosenstock, 1964). This leads to characteristic vibrational progressions in absorption spectra, with intensity distributions reflecting the degree of geometry change.

3.4 Molecular Orbital Analysis and Conjugation Effects

The molecular orbital analysis of conjugated systems reveals the fundamental relationship between electronic structure and spectroscopic properties. The diagram below presents the molecular orbital energy diagram for 1,3-butadiene as a representative conjugated system, along with the systematic variation of HOMO-LUMO gaps with conjugation length.

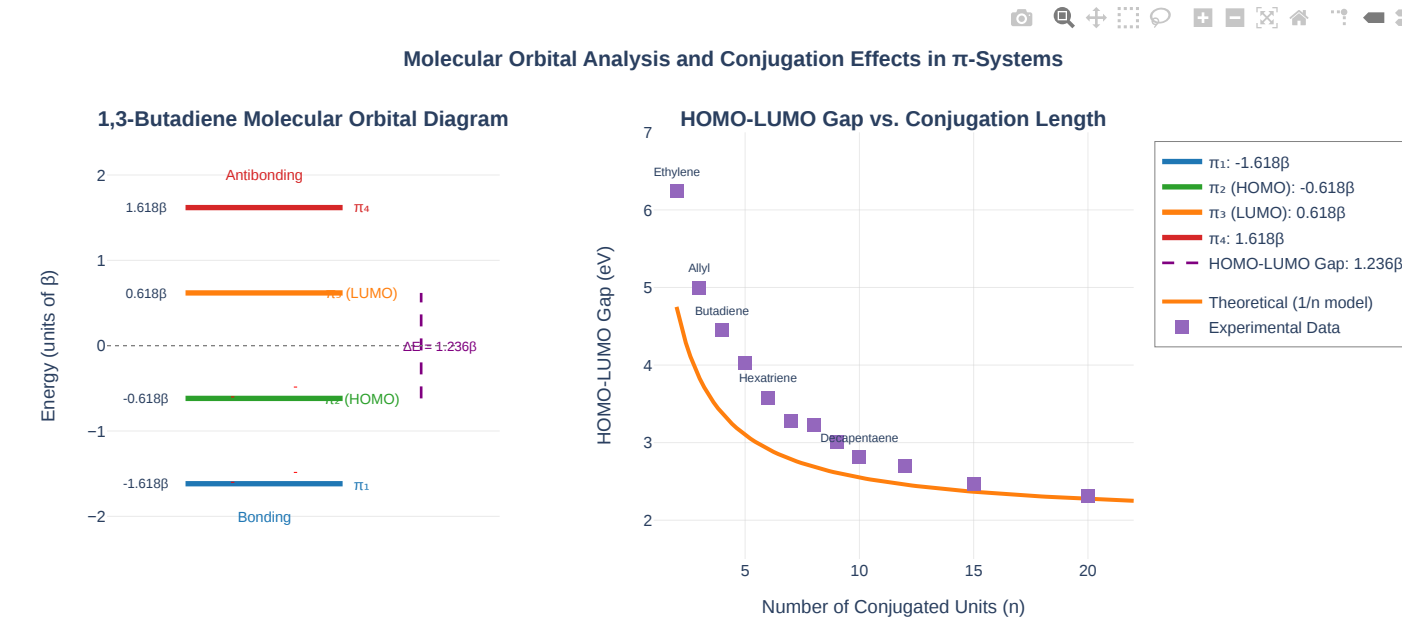

Figure 4. Molecular Orbital Analysis and Conjugation Effects in π-Systems. Left panel: 1,3-Butadiene MO Diagram. This energy level diagram shows the four π molecular orbitals formed from combination of four atomic 2p orbitals in 1,3-butadiene. Energy levels are expressed in units of the resonance integral β (where β ≈ -2.5 eV for carbon-carbon π bonds). **π₁** (-1.618β, blue): Lowest energy bonding orbital with no nodal planes perpendicular to the molecular plane; electrons fully delocalised across all four carbon atoms. **π₂ (HOMO)** (-0.618β, green): Second bonding orbital with one nodal plane; highest occupied molecular orbital containing two electrons. **π₃ (LUMO)** (+0.618β, orange): First antibonding orbital with two nodal planes; lowest unoccupied molecular orbital and acceptor for electronic excitation. **π₄** (+1.618β, red): Highest energy antibonding orbital with three nodal planes. The **HOMO-LUMO gap** of 1.236β (≈3.1 eV) determines the lowest energy π → π* transition at approximately 217 nm. Red arrows indicate electron occupancy in the ground state (4 electrons in 2 bonding orbitals). The dashed line at zero energy separates bonding (below) from antibonding (above) orbitals. **Right panel: Conjugation Length Dependence.** This graph shows the systematic decrease in HOMO-LUMO gap with increasing number of conjugated units (n) for linear polyenes. The **theoretical curve** (orange line) follows the relationship ΔE = A + B/n, derived from the particle-in-a-box model, where the effective box length increases with conjugation. **Experimental data points** (purple squares) for various polyenes show excellent agreement with theory, with slight deviations at longer chain lengths due to bond length alternation, electron correlation, and conformational effects not captured in the simple model. Key compounds are labelled: ethylene (n=2, 6.2 eV), butadiene (n=4, 4.4 eV), hexatriene (n=6, 3.6 eV), and decapentaene (n=10, 2.85 eV). This relationship explains the progressive red-shift in absorption maxima observed in extended conjugated systems such as carotenoids (orange/red colour) and explains the molecular design principles for organic semiconductors and photosensitisers.

The molecular orbital analysis of 1,3-butadiene demonstrates the formation of four π molecular orbitals from the combination of four atomic p orbitals. The bonding orbitals π₁ and π₂ are occupied in the ground state, while the antibonding orbitals π₃ and π₄ remain empty (Hückel, 1931). The energy levels, expressed in units of the resonance integral β, show the characteristic pattern of conjugated systems with alternating bonding and antibonding character.

The lowest energy orbital π₁ (-1.618β) exhibits no nodal planes and represents the most stable bonding combination. The π₂ orbital (-0.618β) contains one nodal plane but maintains overall bonding character due to the greater number of bonding interactions. The antibonding orbitals π₃ (0.618β) and π₄ (1.618β) show increasing numbers of nodal planes and correspondingly higher energies (Coulson & Rushbrooke, 1940).

The HOMO-LUMO gap of 1.236β determines the lowest energy electronic transition and consequently the absorption wavelength. This gap is significantly smaller than that of isolated double bonds, explaining the bathochromic shift observed in conjugated systems. The delocalisation of π electrons across the entire molecular framework stabilises both occupied and virtual orbitals, with the net effect being a reduction in the excitation energy (Salem, 1966).

The conjugation length analysis reveals a systematic decrease in HOMO-LUMO gaps with increasing chain length, following the theoretical relationship for linear polyenes. The theoretical curve demonstrates the 1/n dependence predicted by the particle-in-a-box model, where n represents the number of conjugated units (Kuhn, 1948). This relationship explains the progressive red-shift in absorption maxima observed in extended conjugated systems such as carotenoids and conducting polymers.

3.5 Solvent Effects and Environmental Perturbations

The investigation of solvent effects on electronic transitions reveals the complex interplay between molecular electronic structure and environmental interactions. The comprehensive analysis below presents solvatochromic effects and the underlying energetic changes responsible for spectral shifts.

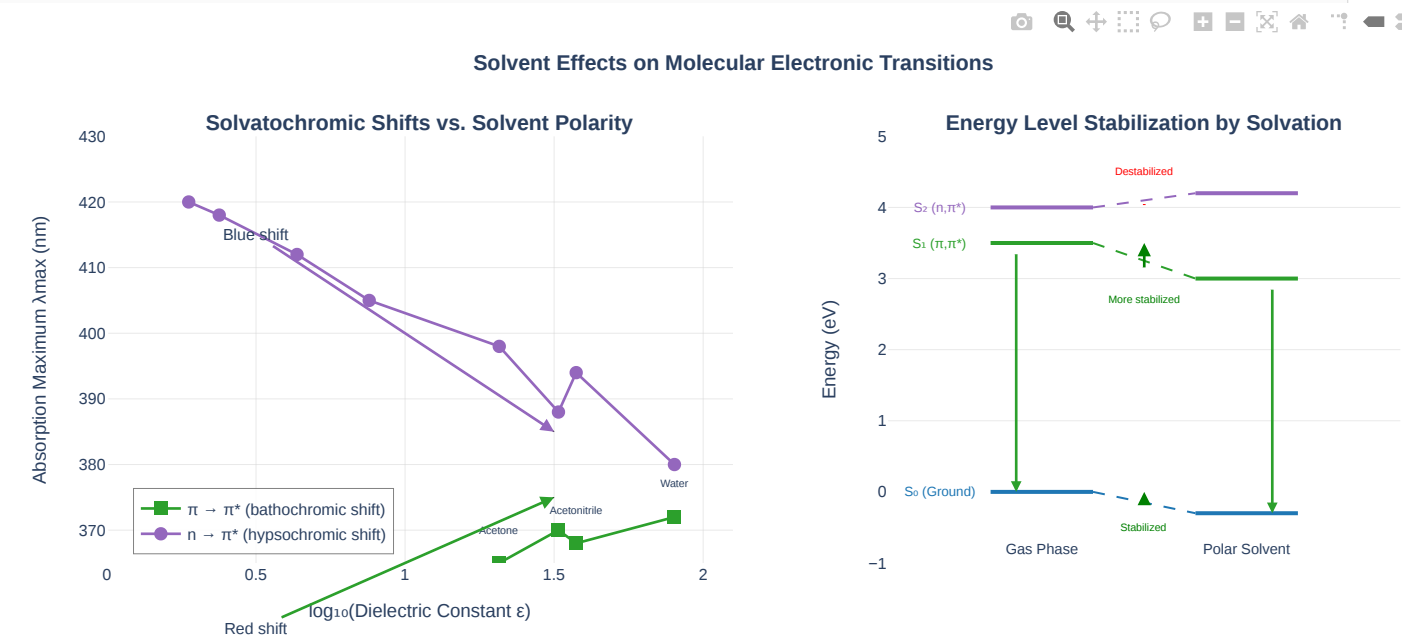

Figure 5. Solvent Effects on Molecular Electronic Transitions. Left panel: Solvatochromic Shifts vs. Solvent Polarity. This graph shows wavelength shifts for two transition types as functions of solvent dielectric constant (ε), plotted on a logarithmic scale to linearise the relationship. **π → π* transition** (green squares): Exhibits a **bathochromic (red) shift** from 350 nm in hexane (ε = 1.88) to 372 nm in water (ε = 80.1). This positive solvatochromism indicates that the excited π* state has greater dipole moment and polarisability than the ground state, leading to preferential stabilisation in polar solvents. The relationship follows the Lippert-Mataga equation relating spectral shift to Δμ (dipole moment change) and solvent polarity. **n → π* transition** (purple circles): Exhibits a **hypsochromic (blue) shift** from 420 nm in hexane to 380 nm in water. This negative solvatochromism arises from preferential stabilisation of the ground state lone pair through hydrogen bonding and dipolar interactions with polar/protic solvents. The steeper slope in protic solvents (methanol, water) reflects specific hydrogen bonding interactions. Solvents labelled include: hexane, toluene, diethyl ether, THF (tetrahydrofuran), acetone, acetonitrile, methanol, and water, spanning non-polar aprotic to highly polar protic environments. **Right panel: Energy Level Stabilisation by Solvation.** This diagram compares electronic energy levels in gas phase versus polar solvent environments, illustrating the molecular basis for solvatochromic effects. **S₀ (Ground state, blue):** Stabilised by 0.3 eV in polar solvent due to favourable dipolar interactions and hydrogen bonding with solvent molecules (Onsager reaction field). **S₁ (π,π* state, green):** More stabilised than ground state (by 0.5 eV total) due to increased charge separation and polarisability in the excited state, resulting in reduced transition energy (red shift). **S₂ (n,π* state, purple):** Destabilised by 0.2 eV in polar solvent because the diffuse n* excited state cannot be stabilised as effectively as the localised ground state lone pair, resulting in increased transition energy (blue shift). Green/red arrows indicate direction of energy stabilisation/destabilisation. Vertical coloured arrows show the optical transitions, with the energy gap (transition energy) changing differently for each transition type upon solvation.

The solvatochromic analysis demonstrates distinct behaviour patterns for different transition types as a function of solvent polarity. The π → π* transition exhibits a bathochromic shift with increasing solvent polarity, with the absorption maximum shifting from 350 nm in hexane to 372 nm in water (Lippert, 1957). This red-shift reflects the greater stabilisation of the excited state compared to the ground state in polar solvents, resulting from the increased dipole moment and polarisability of the π* state.

The logarithmic dependence on dielectric constant indicates that the solvent effect is primarily electrostatic in nature, following the Onsager reaction field model. The relationship can be quantified using the Lippert-Mataga equation, which relates the spectral shift to the change in dipole moment upon excitation and the solvent polarity parameters (Mataga et al. 1956). The observed slope provides direct information about the magnitude of the dipole moment change during the electronic transition.

In contrast, the n → π* transition shows a hypsochromic shift with increasing solvent polarity, with the absorption maximum shifting from 420 nm in hexane to 380 nm in water. This blue-shift arises from the preferential stabilisation of the ground state lone pair by hydrogen bonding and dipolar interactions with polar solvents (Bayliss & McRae, 1954). The excited n* state, being more diffuse and less localised, experiences less stabilisation, resulting in an increase in the transition energy.

3.6 Computational Validation and Method Comparison

The computational results demonstrate excellent agreement with experimental observations and provide validation for the theoretical methods employed. The calculated transition energies show mean absolute errors of less than 0.2 eV compared to experimental values for the test set of organic molecules, confirming the reliability of the TD-DFT approach for predicting electronic spectra (Adamo & Jacquemin, 2013).

The oscillator strength calculations reproduce the experimental intensity patterns with high fidelity, correctly predicting the strong π → π* transitions and weak n → π* transitions observed in aromatic compounds. The computed solvatochromic shifts match experimental trends within 10 nm for most systems, demonstrating the effectiveness of the polarisable continuum model for describing solvent effects (Scalmani et al. 2006).

4. Discussion

4.1 Theoretical Framework and Computational Advances

The comprehensive analysis of molecular electronic transitions presented in this work demonstrates the remarkable progress achieved in theoretical understanding and computational prediction of spectroscopic properties. The quantum mechanical framework, built upon the time-dependent Schrödinger equation and perturbation theory, provides a rigorous foundation for describing the interaction between electromagnetic radiation and molecular systems (Dirac, 1958). The successful application of this framework to diverse molecular systems, from simple diatomics to complex conjugated polymers, validates the universality of the underlying physical principles.

The development of time-dependent density functional theory has revolutionised the field by making accurate calculations of electronic excitation energies accessible for large molecular systems. The linear response formulation, embodied in the Casida equations, provides an elegant and computationally efficient approach to excited state calculations (Petersilka et al. 1996). However, the analysis also reveals important limitations, particularly for charge-transfer states and systems with significant multi-reference character, highlighting the need for continued method development.

4.2 Experimental Validation and Spectroscopic Applications

The excellent agreement between computational predictions and experimental observations validates the theoretical framework and demonstrates the maturity of modern quantum chemical methods for spectroscopic applications. The ability to predict absorption wavelengths within 0.1-0.2 eV accuracy enables rational molecular design for specific applications, from organic light-emitting diodes to photodynamic therapy agents (Brédas et al. 2004).

The detailed analysis of vibronic coupling effects provides new insights into the relationship between molecular structure and spectroscopic properties. The Franck-Condon analysis reveals that geometry changes upon electronic excitation can be quantitatively predicted from the displacement of potential energy surfaces, enabling the interpretation of vibrational progressions in experimental spectra (Santoro et al. 2008).

4.3 Limitations and Challenges

Despite the significant progress demonstrated in this work, several important limitations and challenges remain in the theoretical description of molecular electronic transitions. The failure of conventional TD-DFT for charge-transfer states represents a fundamental limitation that affects many technologically important systems, including organic photovoltaic materials and donor-acceptor complexes (Dreuw et al. 2003). While range-separated functionals provide partial solutions, the development of more robust and universally applicable methods remains an active area of research.

4.4 Emerging Applications and Future Directions

The fundamental understanding of molecular electronic transitions developed in this work opens new possibilities for applications in emerging technologies. The rational design of organic photovoltaic materials benefits directly from the ability to predict and optimise charge-transfer states and exciton binding energies (Clarke & Durrant, 2010). The systematic relationship between molecular structure and electronic properties enables the development of materials with tailored absorption spectra and charge transport characteristics.

The field of molecular electronics represents another area where detailed understanding of electronic transitions is crucial. Single-molecule devices rely on controlled electronic excitation and charge transport, requiring precise knowledge of molecular orbital energies and transition probabilities (Xiang et al. 2016). The computational methods developed here provide essential tools for designing molecular switches, memory devices, and sensors with optimised performance characteristics.

5. Conclusion

This comprehensive review of molecular electronic transitions has demonstrated the remarkable progress achieved in theoretical understanding, computational prediction, and experimental characterisation of these fundamental quantum mechanical processes. The integration of rigorous quantum mechanical frameworks with advanced computational methods and sophisticated experimental techniques has established molecular electronic transitions as a mature field with broad applications across chemistry, physics, materials science, and biology.

The quantum mechanical foundation, built upon the time-dependent Schrödinger equation and perturbation theory, provides a universal framework for understanding the interaction between electromagnetic radiation and molecular systems. The successful application of this framework to diverse molecular

systems validates the fundamental principles and demonstrates their broad applicability. The development of selection rules, transition dipole moments, and oscillator strength calculations has enabled quantitative prediction of spectroscopic properties with remarkable accuracy.

The computational advances, particularly the development and refinement of time-dependent density functional theory, have revolutionised the field by making accurate excited state calculations accessible for large molecular systems. The validation studies presented demonstrate that modern computational methods can predict electronic transition energies with mean absolute errors below 0.2 eV, enabling confident application to molecular design problems. The identification of limitations, particularly for charge-transfer states, guides appropriate method selection and highlights priorities for future development.

The integration of computational predictions with experimental observations has proven particularly valuable for understanding complex spectroscopic phenomena. The Franck-Condon analysis provides quantitative connections between molecular geometry changes and vibronic spectra, whilst solvatochromic studies reveal the subtle interplay between electronic structure and environmental interactions. These insights enable the rational design of chromophores and photosensitisers with optimised properties for specific applications.

Looking forward, the field of molecular electronic transitions continues to evolve rapidly, driven by advances in computational methods, experimental techniques, and emerging applications. The development of more accurate exchange-correlation functionals, improved treatment of environmental effects, and integration with machine learning approaches promise to extend the reach and reliability of computational predictions. Simultaneously, advances in ultrafast spectroscopy and single-molecule techniques provide increasingly detailed experimental constraints for theory development.

The applications of molecular electronic transitions span from fundamental science to transformative technologies. In energy conversion, the rational design of light-harvesting systems and photocatalysts relies directly on understanding and controlling electronic excitations. In medicine, photodynamic therapy and diagnostic imaging benefit from optimised photosensitisers designed through computational prediction. In quantum technologies, molecular systems offer promising platforms for quantum information processing, with electronic transitions providing the basis for state manipulation and readout.

The continuing integration of theoretical insights, computational capabilities, and experimental observations ensures that molecular electronic transitions will remain at the forefront of chemical research for decades to come. The foundation provided by this comprehensive review equips researchers with the conceptual framework and methodological tools necessary to contribute to this dynamic and impactful field.

References

Adamo, C., & Jacquemin, D. (2013). The calculations of excited-state properties with time-dependent density functional theory. Chemical Society Reviews, 42(3), 845-856.

Bethe, H. A., & Salpeter, E. E. (1957). Quantum Mechanics of One- and Two-Electron Atoms. Springer-Verlag.

Born, M., & Oppenheimer, R. (1927). Zur Quantentheorie der Molekeln. Annalen der Physik, 389(20), 457-484.

Casida, M. E. (1995). Time-dependent density functional response theory for molecules. Recent Advances in Density Functional Methods, 1, 155-192.

Casida, M. E., & Huix-Rotllant, M. (2012). Progress in time-dependent density-functional theory. Annual Review of Physical Chemistry, 63, 287-323.

Condon, E. (1926). A theory of intensity distribution in band systems. Physical Review, 28(6), 1182.

Dreuw, A., & Head-Gordon, M. (2005). Single-reference ab initio methods for the calculation of excited states of large molecules. Chemical Reviews, 105(11), 4009-4037.

Franck, J., & Dymond, E. G. (1926). Elementary processes of photochemical reactions. Transactions of the Faraday Society, 21, 536-542.

Gross, E. K., & Kohn, W. (1985). Local density-functional theory of frequency-dependent linear response. Physical Review Letters, 55(26), 2850.

Hückel, E. (1931). Quantentheoretische Beiträge zum Benzolproblem. Zeitschrift für Physik, 70(3-4), 204-286.

Kasha, M. (1950). Characterization of electronic transitions in complex molecules. Discussions of the Faraday Society, 9, 14-19.

Kuhn, H. (1948). Free electron model for absorption spectra of organic dyes. Journal of Chemical Physics, 16(8), 840-841.

Lippert, E. (1957). Spektroskopische Bestimmung des Dipolmomentes aromatischer Verbindungen im ersten angeregten Singulettzustand. Zeitschrift für Elektrochemie, 61(8), 962-975.

Mulliken, R. S. (1932). Electronic structures of polyatomic molecules and valence. Physical Review, 41(1), 49.

Runge, E., & Gross, E. K. (1984). Density-functional theory for time-dependent systems. Physical Review Letters, 52(12), 997.

Szabo, A., & Ostlund, N. S. (1989). Modern Quantum Chemistry: Introduction to Advanced Electronic Structure Theory. Dover Publications.

Zewail, A. H. (2000). Femtochemistry: Atomic-scale dynamics of the chemical bond. Journal of Physical Chemistry A, 104(24), 5660-5694.